Microfluidics and Nanofluidics (2019) 23:41
https://doi.org/10.1007/s10404-019-2204-3

RESEARCH PAPER

Dean-flow-coupled elasto-inertial particle and cell focusing in symmetric serpentine microchannels

Dan Yuan[1] · Ronald Sluyter[2,3] · Qianbin Zhao[1] · Shiyang Tang[1] · Sheng Yan[4] · Guolin Yun[1] · Ming Li[5] · Jun Zhang[6] · Weihua Li[1]

Received: 16 November 2018 / Accepted: 6 February 2019 / Published online: 21 February 2019

Abstract

This work investigates particle focusing under Dean-flow-coupled elasto-inertial effects in symmetric serpentine microchannels. A small amount of polymers were added to the sample solution to tune the fluid elasticity, and allow particles to migrate laterally and reach their equilibriums at the centerline of a symmetric serpentine channel under the synthesis effect of elastic, inertial and Dean-flow forces. First, the effects of the flow rates on particle focusing in viscoelastic fluid in serpentine channels were investigated. Then, comparisons with particle focusing in the Newtonian fluid in the serpentine channel and in the viscoelastic fluid in the straight channel were conducted. The elastic effect and the serpentine channel structure could accelerate the particle focusing as well as reduce the channel length. This focusing technique has the potential as a pre-ordering unit in flow cytometry for cell counting, sorting, and analysis. Moreover, focusing behaviour of Jurkat cells in the viscoelastic fluid in this serpentine channel was studied. Finally, the cell viability in the culture medium containing a dissolved polymer and after processing through the serpentine channel was tested. The polymer within this viscoelastic fluid has a negligible effect on cell viability.

Keywords Viscoelastic fluid · Dean-flow-coupled elasto-inertial effects · Viscoelastic force · Cell viability

1 Introduction

Microfluidic particle focusing has been widely applied in numerous biomedical and chemical applications (Gossett et al. 2010; Pamme 2007; Sajeesh and Sen 2014), since it is an essential step for downstream particle separation (Whitesides 2006a; Yuan et al. 2017b, 2015), counting (Bhagat et al. 2010), detection, or analysis (Nam et al. 2016; Nitta et al. 2018; Yuan et al. 2016a). Particle focusing has been extensively studied in the Newtonian fluid using active and passive methods (Khoo et al. 2018; Vaidyanathan et al. 2018; Whitesides 2006b; Zhang et al. 2016). Active methods, such as dielectrophoresis (DEP) (Kang et al. 2008; Yan et al. 2014), magnetophoresis (Hejazian et al. 2015; Zeng et al. 2012), acoustophoresis (Heyman 1993), and optical tweezers (MacDonald et al. 2003), are based on the external force fields. Whereas passive methods rely on intrinsic hydrodynamic forces induced in microchannels with specialized geometry or structures (Augustsson et al. 2009; Morton et al. 2008; Yang et al. 2007), such as pinched flow fractionation (PFF) (Yamada et al. 2004), hydrodynamic filtration (Crowley and Pizziconi 2005), inertial microfluidics

This article is part of the topical collection "Particle motion in non-Newtonian microfluidics" guest edited by Xiangchun Xuan and Gaetano D'Avino

✉ Jun Zhang
jun.zhang@griffith.edu.au

✉ Weihua Li
weihuali@uow.edu.au

[1] School of Mechanical, Materials, Mechatronic and Biomedical Engineering, University of Wollongong, 2522 Wollongong, NSW, Australia

[2] School of Biological Sciences, University of Wollongong, Wollongong, NSW 2522, Australia

[3] Illawarra Health and Medical Research Institute, Wollongong, NSW 2522, Australia

[4] Department of Chemistry, University of Tokyo, Tokyo, Japan

[5] School of Engineering, Macquarie University, Sydney, NSW 2122, Australia

[6] Queensland Micro and Nanotechnology Centre, Griffith University, Brisbane, QLD 4111, Australia

(Di Carlo 2009; Kuntaegowdanahalli et al. 2009), and deterministic lateral displacement (DLD) (Davis et al. 2006).

The above microfluidic methods for particle focusing are all performed in Newtonian fluids, which employ either external force fields or specially designed complex channels. Recently, there is increasing research interest on particle manipulation in viscoelastic fluids because of its superior focusing performance and simpler channel design (D'Avino et al. 2017; D'Avino and Maffettone 2015; Faridi et al. 2017; Lu et al. 2017; Yuan et al. 2017a, 2016b, 2018). The viscoelastic particle focusing has been investigated extensively in straight channels with cylindrical (D'Avino et al. 2012; Kang et al. 2013; Seo et al. 2014) and rectangular cross sections (Leshansky et al. 2007; Liu et al. 2017; Xiang et al. 2016a; Yang et al. 2011), spiral microchannels (Lee et al. 2013; Liu et al. 2016; Xiang et al. 2016b) and straight channel with side walls (Cha et al. 2014; Yuan et al. 2015).

This work aimed to investigate particle focusing under Dean-flow-coupled elasto-inertial effects in a serpentine microchannel. A small amount of polymers were added to the sample solution to allow particles to migrate laterally and reach equilibrium at the centreline of channel under the synthesis effect of elastic, inertial and Dean-flow forces. First, the effects of the flow rates on particle viscoelastic focusing in serpentine channels were investigated. Then, comparisons with particle focusing in the Newtonian fluid in the serpentine channel and in the viscoelastic fluid in the straight channel were conducted. It was found that the elastic effect plays an important role in efficient particle focusing, and the serpentine channel structure could accelerate the particle focusing as well as reduce the channel length. This focusing technique has the potential as a pre-ordering unit in flow cytometry for cell counting, sorting, and analysis. In addition, the focusing behaviour of human Jurkat cells in the viscoelastic fluid in this serpentine channel, as well as the cell viability in poly(ethylene oxide) (PEO) dissolved cell culture medium and in PEO dissolved PBS before and after microfluidic processing was tested. To the best knowledge of the authors, this is the first time that the biocompatibility of dissolved PEO polymer on cells in microfluidic focusing experiments has been reported.

2 Theory

2.1 Elastic force

In viscoelastic fluid, the polymer within the medium can induce an additional elastic force on particles. W_i was used to characterize the elastic effects of the viscoelastic fluid, which is the ratio of two time constants (Yang et al. 2011):

$$W_i = \frac{\lambda}{t_\mathrm{f}} = \lambda\dot{\gamma} = \lambda\frac{2V_\mathrm{m}}{w} = \frac{2\lambda Q}{hw^2}, \tag{1}$$

where λ defines the relaxation time of the fluid, and V_m and t_f define the average velocity and characteristic time of the channel flow, respectively. The characteristic time is $2V_\mathrm{m}/w$ or $2\lambda Q/hw^2$ in a rectangular channel. In viscoelastic fluids, both the first normal stress N_1 $(=\tau_{xx}-\tau_{yy})$ and the second normal stress N_2 $(=\tau_{yy}-\tau_{zz})$ contribute to particle migration. τ_{xx}, τ_{yy}, and τ_{zz} are normal stresses that are exerted in the flow, for the velocity gradient and vorticity direction, respectively. However, the effects of N_2 can be neglected in the diluted polyethylene oxide (PEO) solutions (Magda et al. 1991; Pathak et al. 2004), because N_1 is much larger than N_2. The elastic force F_E, which originates from an imbalance in the distribution of $N_1(=\tau_{xx}-\tau_{yy})$ over the size of the particle, can be expressed as (Lu et al. 2017):

$$F_\mathrm{E} = C_\mathrm{eL}a^3\nabla N_1 = C_\mathrm{eL}a^3(\nabla\tau_{xx}-\nabla\tau_{yy}) = -2C_\mathrm{eL}a^3\eta_\mathrm{p}\lambda\nabla\dot{\gamma}^2, \tag{2}$$

where C_eL is the non-dimensional elastic lift coefficient, a is the particle size, and η_p is the polymeric contribution to the solution viscosity.

3 Drag force

Assuming a spherical particle travelling in a uniform Stokes fluid, and there is a velocity difference between particle and fluid, a drag force can arise, which can be expressed as (Di Carlo 2009; Zhang et al. 2016)

$$F_\mathrm{D} = 3\pi\mu_f a(v_\mathrm{f}-v_\mathrm{p}), \tag{3}$$

where v_f and v_p are the velocities of the fluid element and particles, respectively, a is the particle size, and μ_f represents the fluid viscosity.

3.1 Schematic of the Dean-flow-coupled elasto-inertial particle focusing in symmetric serpentine channel

When particles in viscoelastic fluid flow in a symmetric serpentine channel under a certain flow rate, the particles are experiencing three forces: inertial lift force F_L, the resultant of the shear-gradient lift force (F_LS), and wall-repulsion force (F_LW); the Dean drag force F_D, resulting from the curved channel geometry; and elastic force F_E, induced by the nature of the viscoelastic medium. When particles in Newtonian fluid flow in straight channels, the shear gradient lift force pushes particles away from the centreline of the channel, while the wall lift force drives particles away from the channel wall. When the particles are not in straight channels but in a symmetric serpentine channel with a Newtonian fluid, two counter-rotating vortices are generated due to the non-uniform inertia of fluid elements within the channel cross section. Therefore, the Dean drag force, which is

perpendicular to the particle velocity, directing from the inner corner to the outer corner, acts in superposition on the particles, and the trajectory of these particles can be confined within a certain width after a certain distance. However, when particles are in the viscoelastic fluid, rather than Newtonian fluid, in a symmetric serpentine channel, the viscoelastic force F_E should arise, which is directing away from the wall and declining with increasing distance from the wall. After introduction of the elastic force, the particle focusing can be improved. Compared with particle focusing in the Newtonian fluid in the serpentine channel, the addition of elastic force can accelerate the focusing process, as well as improve the focusing performance. With the synergetic effect of inertial lift force F_L, the Dean drag force F_D, and elastic force F_E, the Dean-flow-coupled elasto-inertial particle focusing in symmetric serpentine channels can be realized easily in a relatively short length, Fig. 1.

4 Materials and methods

4.1 Design and fabrication of a microfluidic device

Standard photolithography and soft lithographic techniques were used to fabricate the following device (McDonald and Whitesides 2002; Sollier et al. 2011). The symmetric serpentine channel consisted of a 20 mm serpentine section with 16 zigzag periods. The width of micro-channel was 100 μm. The depth of the channel was uniform at 42 μm. As a comparison, a straight channel with the same width and height (100 μm × 45 μm) but with longer length (40 mm) was used to investigate the effect of serpentine structure on particle focusing.

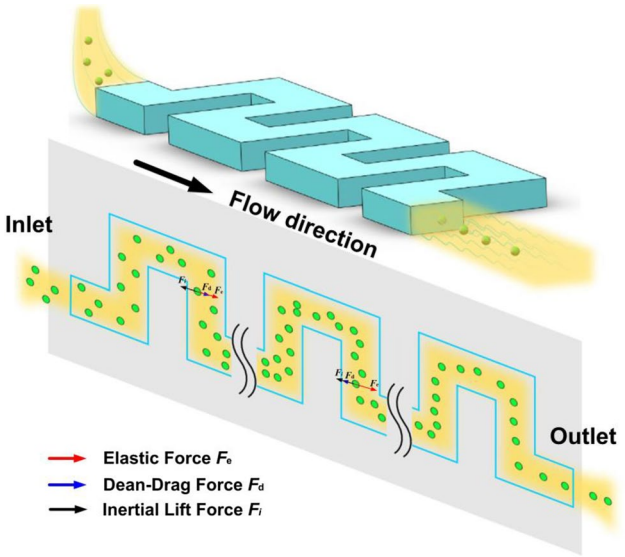

Fig. 1 Schematic view of the Dean-flow-coupled elasto-inertial particle focusing in the serpentine channels

4.2 Preparation of the PEO medium

For particle focusing, PEO (2,000,000 Da; Sigma-Aldrich) was dissolved in deionized water (DI water) with a concentration of 1000 ppm to form the viscoelastic fluid. For comparisons to Newtonian fluid, the fluid was DI water. Tween 20 (Sigma-Aldrich) was added to DI water with a volume ratio of 0.01% (v/v) to prevent particle aggregation.

For Jurkat cell viability test, PEO was dissolved in cell culture medium [Roswell Park Memorial Institute (RPMI) 1640 medium (Thermo Fisher Scientific) containing 10% fetal bovine serum (Bovogen Biologicals) and 2 mM L-glutamine (Thermo Fisher Scientific)] at various concentrations. For Jurkat cell viscoelastic focusing and viability testing before and after each experiment, PEO was dissolved in phosphate-buffered saline (PBS) with a concentration of 1000 ppm.

4.3 Particle and cell preparation

For particle focusing experiments, particle suspensions were prepared by diluting 13 μm internally red dyed fluorescent polystyrene microspheres (Thermo Fisher Scientific, CV5%) in the 1000 ppm PEO medium.

For cell focusing and viability tests, Jurkat cells (ATCC), an immortalized human leukaemic T cell line (average diameter of approximately 15 μm), were cultured in complete (RPMI) 1640 medium in a humidified incubator (Thermo Scientific) at 37 °C and 95% air/5% CO_2. Before commencing each experiment, the particle mixture was re-suspended by vortexing and cell samples were manually stirred to provide uniform suspensions in a complete medium containing PEO.

4.4 Cell viability test

Live cells have intact membranes that exclude a variety of dyes that easily penetrate the damaged, permeable membranes of non-viable cells. In cell viability tests (including the viability tests of Jurkat cells in a polymer dissolved cell culture medium with different PEO concentrations after incubation, and before and after the viscoelastic microfluidic experiment), fluorochrome 7-amino actinomycin D (7-AAD) (Thermo Scientific) was used to stain non-viable cells. 1 μl 7AAD was added to each 300 μl Jurkat cell sample, and after 30 s, the 7-AAD fluorescence was determined by flow cytometry (BD Accuri C6, BD biosciences). Therefore, the number of viable and non-viable cells can be analyzed based on the 7-AAD fluorescence.

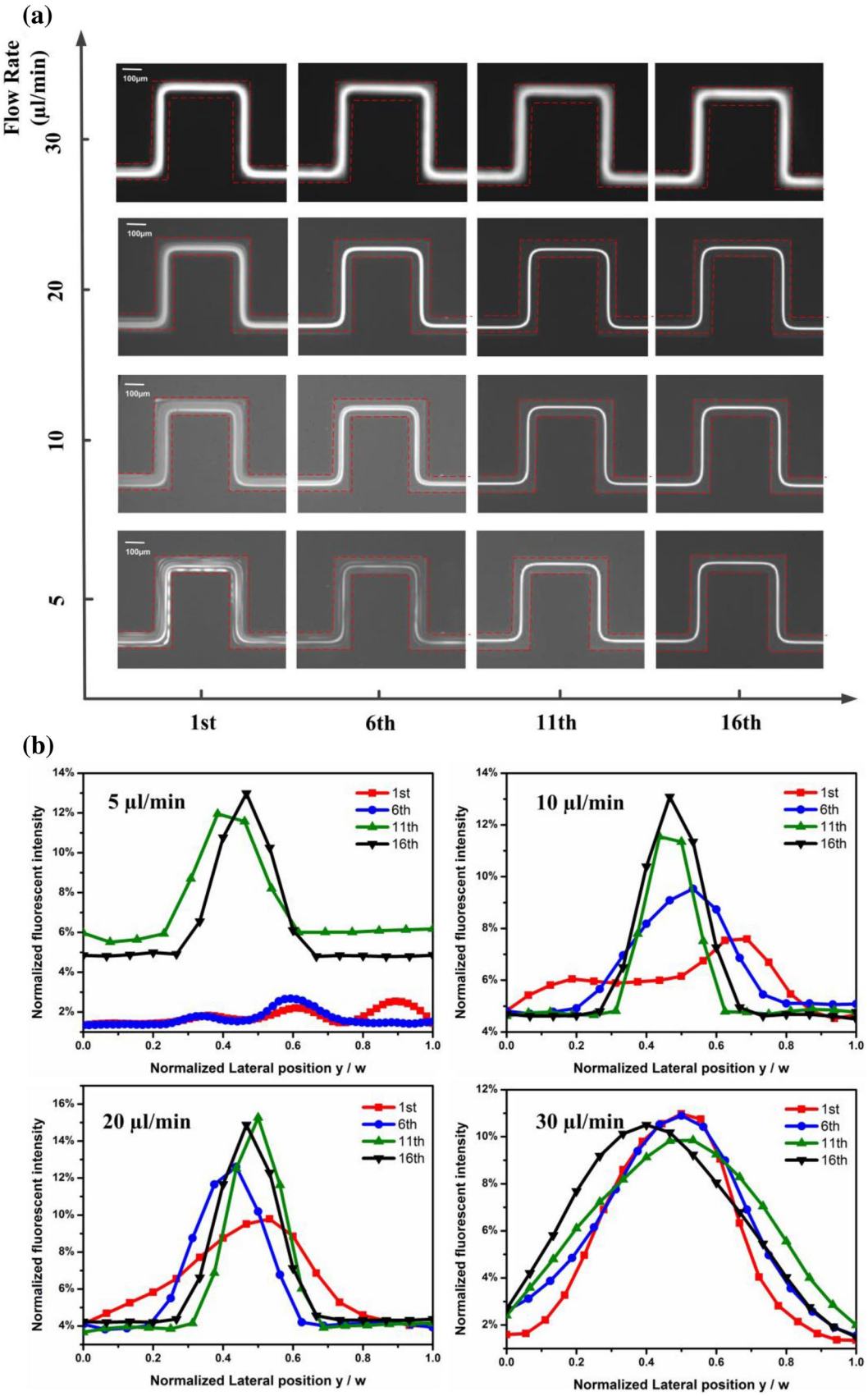
(a)
Flow Rate (μl/min)
30
20
10
5
100μm
1st
6th
11th
16th
(b)
5 μl/min
10 μl/min
20 μl/min
30 μl/min
1st
6th
11th
16th
Normalized fluorescent intensity
Normalized Lateral position y / w

◂**Fig. 2** Effects of flow rate on particle viscoelastic focusing in the serpentine channel. **a** Fluorescent images of particle focusing at different zigzag turns under different flow rates. **b** Fluorescent intensity profile at the middle of each zigzag turn under different flow rates (as indicated)

4.5 Experimental setup

The sample suspension was transferred to the chip from two 1 ml syringes, with silicon tube connected between them. The flow rate was controlled by syringe pumps (Legato 100, Kd Scientific, USA). An inverted microscope (CKX41, Olympus, Japan) mounted with a CCD camera (Optimos, Q-imaging, Australia) was used to observe and capture images of the fluorescent particles, cells and fluids. The fluorescent images were post-processed and analyzed with Q-Capture Pro 7 (Q-imaging, Australia) software.

5 Results and discussion

5.1 Effect of flow rates

Figure 2 shows the 13 μm particle distribution along the channel length from the 1st zigzag turn to the 16th zigzag turn under different flow rates. As seen from the fluorescent images of particle focusing (Fig. 2a), when the flow rate ranges from 5 μl/min to 20 μl/min, the particles can be focused to a single line at the last zigzag turn under the effect of Dean-flow-coupled elasto-inertial effects. As the flow rate increases to 30 μl/min, the particles become dispersed, which is attributed to the fact that inertial effects become dominant gradually. Besides, the channel length for particles to reach a single line is different for flow rates of 5 μl/min, 10 μl/min and 20 μl/min. Among the three flow rates, particles flowing at 20 μl/min first reach their equilibrium positions after the 6th zigzag turn. This indicates that 20 μl/min is the optimal flow rate for particle focusing and this flow rate yields the shortest channel length. Furthermore, as the channel length increases, the particle focusing performance can be improved. Figure 2b shows the corresponding fluorescent intensity profiles at the middle of each zigzag turn under different flow rates. Therefore, it is concluded that as the channel length increases, the focusing performance improves; as the flow rate increases, but below 30 μl/min, the particles are focused more quickly; as the flow rate increases to 30 μl/min or above, the particle focusing is broken by the increasing inertial effects.

5.2 Effect of elasticity

To investigate the fluid elasticity on particle migration, experiments were also carried out in the Newtonian fluid in this serpentine channel. Figure 3 shows the 13 μm particle focusing in the Newtonian fluid in a serpentine channel under the flow rate of 5 μl/min, 10 μl/min, 20 μl/min, and 30 μl/min at the 16th zigzag turn and corresponding fluorescence intensity profiles. The particles remain dispersed under all flow conditions. Compared with particle flowing conditions in Fig. 2, the only difference is the carrying medium. In viscoelastic fluid, the particles can be focused under the synthesis effects of elastic, inertial and Dean-flow forces, while in Newtonian fluid the particles cannot be focused under the effects of inertial and Dean-flow forces. This indicates that the elastic effect plays an important role in efficient particle focusing.

5.3 Effect of Dean flow induced by zigzag turns in the symmetric serpentine channel

To investigate the effects of Dean flow induced by zigzag turns in symmetric serpentine channel, the 13 μm particle distribution in a straight rectangular channel in the same viscoelastic fluid with a cross section of 100 μm × 50 μm (width × height) (Fig. 4) was compared with that in the serpentine channel (Fig. 2). The sole difference between the two channels is the structure. With the zigzag turns, at 20 μl/min, the particles are focused into a single line at centerline under the combined effect of Dean-flow-coupled elasto-inertial effects, while in straight channels, without the Dean-flow effect, the single line focusing cannot be achieved. The particles are dispersed widely at 20 mm from the inlet, and have multiple focusing positions at 30 mm and 40 mm, evidenced by the fluorescent intensity profiles (Fig. 4). In comparison, the total length of the serpentine channel is 20 mm, and the particles are focused at the 6th zigzag turns under the same flow rate and viscoelastesity. This indicates that this serpentine channel allows efficient particle focusing in the viscoelastic fluid with the aid of Dean flow.

5.4 Cell viability test

Figure 5 shows the viability of Jurkat cells in cell culture medium containing polymer PEO, with PEO concentrations of 500 ppm and 1000 ppm after 2 h and 4 h incubation, compared to Jurkat cells in cell culture medium alone (0 ppm). The viability of Jurkat cells in 0 ppm, 500 ppm and 1000 ppm PEO dissolved in cell culture medium was similar at each time point, with no reduction in viability observed for up to 4 h incubation. Thus, PEO has little effect on Jurkat cell viability within 4 h of exposure, displaying high biocompatibility over this time period. This allows sufficient time for carrying out viscoelastic focusing or separation experiments, as well as potential downstream analysis.

After establishing that PEO has negligible effects on Jurkat cell viability, Jurkat cell migration behaviour in

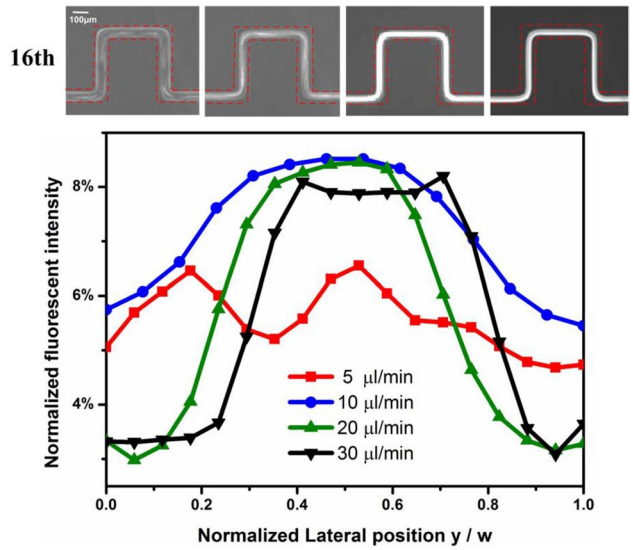

Fig. 3 Particle focusing in Newtonian fluid in serpentine channel under flow rates of 5 μl/min, 10 μl/min, 20 μl/min, and 30 μl/min at the 16th zigzag turn and corresponding fluorescence intensity profiles

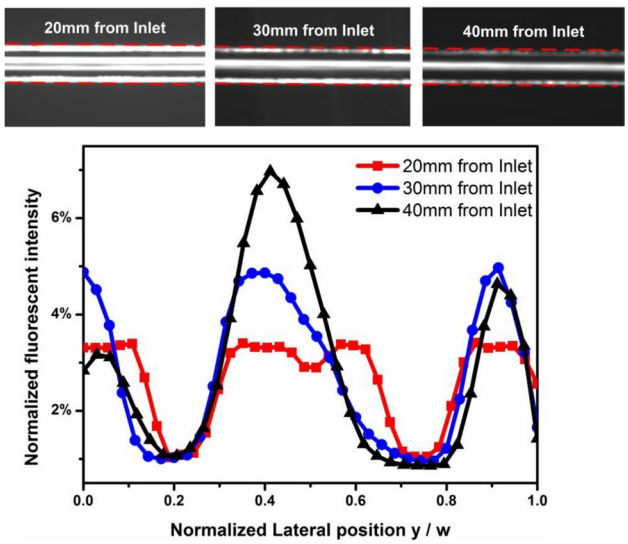

Fig. 4 Particle focusing in a viscoelastic fluid in a straight channel under a flow rate of 20 μl/min

viscoelastic fluids in the serpentine channel, as well as cell viability before and after microfluidic experiments were investigated (Fig. 6). PBS containing polymer (1000 ppm) was used in place of cell culture medium containing the polymer (since most of the microfluidic experiments involving cells are performed in PBS based fluid). The Jurkat cell distribution at the outlet of the serpentine channel under different flow rates was captured and shown in Fig. 6a. At flow rates of 5 μl/min and 10 μl/min, cells were focused to a single line after the 16th zigzag turn, flowing as single events

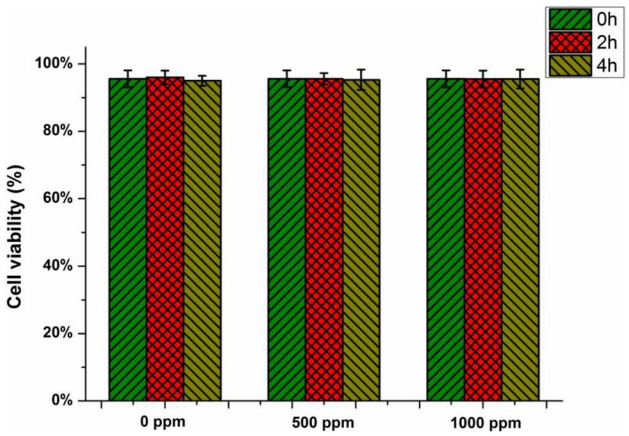

Fig. 5 Cell viability test in polymer dissolved cell culture medium with respect to different culture time and polymer (PEO) concentration

under the Dean-flow-coupled elasto-inertial effects. As the flow rate increases to 20 μl/min or higher, the cells could not be focused well and started to disperse due to the increasing inertial effects. Notably, the optimal focusing flow rates for particles and Jurkat cells are different, despite the Jurkat cells being similar in shape and size to the 13 μm particles. The may be attributed to the differences in deformability of polystyrene particles and cells.

The cell viability was tested before and after the microfluidic focusing experiments (Fig. 6b). The focusing experiments took approximately 1 h. Cell viability was tested in PEO dissolved PBS medium before the experiment at 0 h from the inlet for comparison (the left figure), at approximately 1 h from the inlet (the middle figure), and 1 h from the outlet after focusing experiment (the right figure). The viabilities were 88.6%, 84.7% and 76.7% for cells before the experiment at 0 h from the inlet, 1 h from the inlet, and 1 h from the outlet after focusing experiment, respectively. It can be seen that without running the microfluidic experiment, Jurkat cell viability was reduced slightly from 88.6 to 84.7% after 1 h exposure to PEO polymer in PBS medium. After the cell focusing experiment, the cell viability was reduced further slightly from 84.7 to 76.7% compared to cells not subject to the microfluidic experiments at corresponding time points. This reduction in viability may be due to the mechanical forces that cells experienced during the microfluidic channels rather than exposure to the polymer dissolved in PBS.

From the viability tests of Jurkat cells in polymer dissolved cell culture medium with different PEO concentrations after incubation, and before and after the viscoelastic microfluidic experiment, we concluded that dissolved polymer has a negligible effect on cell viability. Some other researchers have tested the cell viability in other polymer dissolved mediums. Cha et al. (2012) tested whether PVP affects the viability of

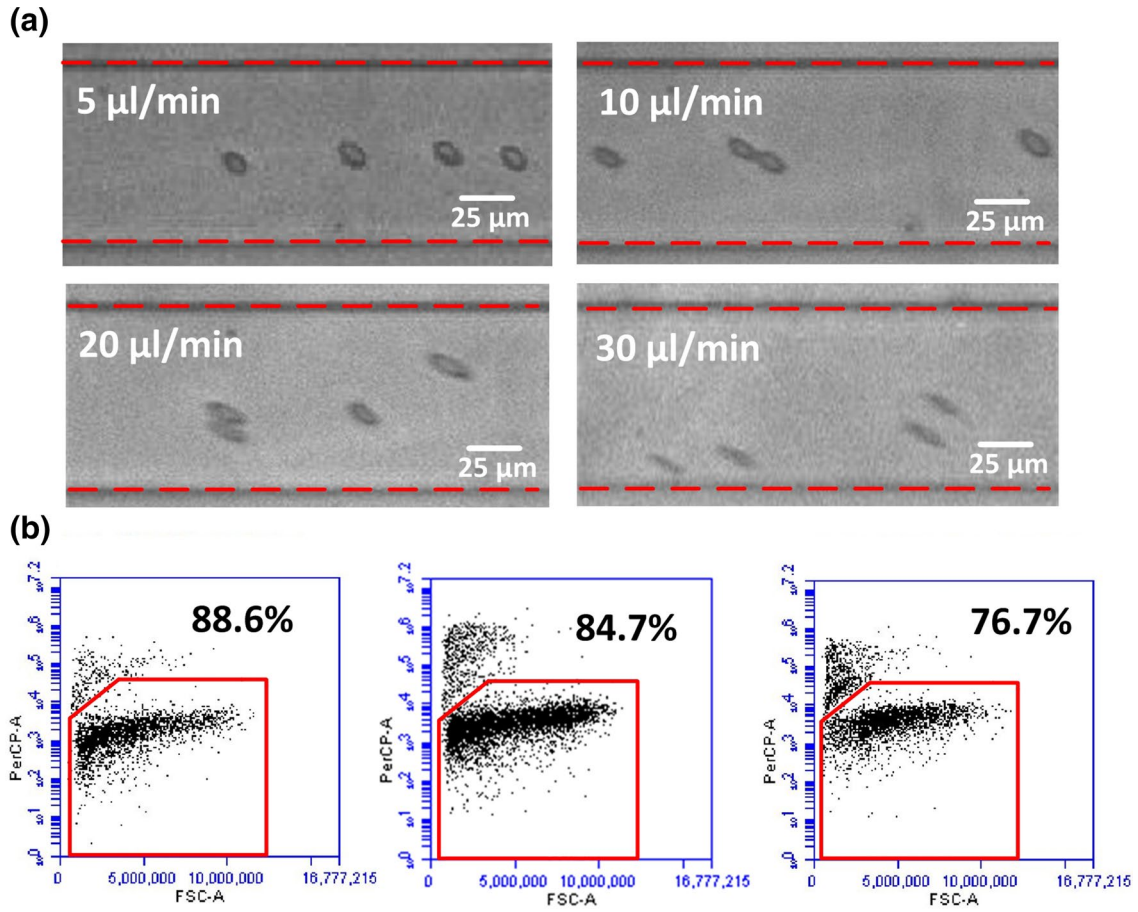

Fig. 6 Jurkat cell focusing in the PEO viscoelastic fluid in a serpentine channel. **a** Jurkat cell focusing in the viscoelastic fluid in a serpentine channel under the effect of different flow rates. **b** Cell viability test before and after viscoelastic microfluidic focusing experiments

the stem cells by MTS assay. The results clearly showed no distinctive difference in viability between the PVP solution and PBS without PVP after 24 h; Besides, Del Giudice et al. (2017) evaluated the viability of both Jurkat and NIH 3T3 cells in aqueous HA 0.8 wt % and without PBS, over 90 min, Cell viability for both cell types in HA 0.8 wt % does not change significantly within 90 min. In our experiments, cell viability test in the polymer dissolved cell culture medium with respect to different culture time (0 h, 2 h, 4 h) and polymer (PEO) concentration (0 ppm, 500 ppm, 1000 ppm), as well as in polymer dissolved PBS before and after viscoelastic microfluidic focusing experiments were examined. To the best knowledge of the authors, this is the first time that the biocompatibility of dissolved PEO polymer on cells in microfluidic focusing experiments has been reported.

6 Concluding remarks

Particle and cell distribution in a symmetric serpentine microchannel in the viscoelastic fluid was investigated. Under Dean-flow-coupled elasto-inertial effects, particles and cells can be focused into a single line. From the experiments of effects of the flow rates on particle/cell focusing, it is concluded that as the flow rate exceeds its optimal focusing value, the inertial effect becomes dominant and disrupts particle focusing. Comparison of particle focusing in the Newtonian fluid in the symmetric serpentine channel, and in the viscoelastic fluid in the straight channel demonstrated the fluid elasticity and Dean flow induced by zigzag turns in the serpentine channel both play important

roles in efficient particle focusing. This focusing technique has the potential as a pre-ordering unit in flow cytometry for cell counting, sorting, and analysis. In addition, the Jurkat cell viability test in the polymer dissolved in cell culture medium, and the cell viability before and after microfluidic experiments indicated that the dissolved PEO polymer within the viscoelastic fluid has minimal effect on cell viability, while the microfluidic focusing may have a minor negative effect on cell viability. The cell viability tests with regard to polymer in viscoelastic fluid provide general information regarding the biocompatibility of the polymer PEO in aqueous solutions.

Acknowledgements This work is supported by the National Natural Science Foundation of China (Grant no. 51705257), the Australian Research Council (ARC) Discovery Project (Grant no. DP180100055), and the Natural Science Foundation of Jiangsu Province (Grant no. BK20170839).

Compliance with ethical standards

Conflict of interest The authors have declared no conflict of interest.

References

Augustsson P, Åberg LB, Swärd-Nilsson A-MK, Laurell T (2009) Buffer medium exchange in continuous cell and particle streams using ultrasonic standing wave focusing. Microchim Acta 164:269–277

Bhagat AAS, Kuntaegowdanahalli SS, Kaval N, Seliskar CJ, Papautsky I (2010) Inertial microfluidics for sheath-less high-throughput flow cytometry. Biomed Microdevices 12:187–195

Cha S et al (2012) Cell stretching measurement utilizing viscoelastic particle focusing. Anal Chem 84:10471–10477

Cha S, Kang K, You JB, Im SG, Kim Y, Kim JM (2014) Hoop stress-assisted three-dimensional particle focusing under viscoelastic flow. Rheol Acta 53:927–933

Crowley TA, Pizziconi V (2005) Isolation of plasma from whole blood using planar microfilters for lab-on-a-chip applications. Lab Chip 5:922–929

D'Avino G, Maffettone P (2015) Particle dynamics in viscoelastic liquids. J Non Newtonian Fluid Mech 215:80–104

D'Avino G, Romeo G, Villone MM, Greco F, Netti PA, Maffettone PL (2012) Single line particle focusing induced by viscoelasticity of the suspending liquid: theory, experiments and simulations to design a micropipe flow-focuser. Lab Chip 12:1638–1645

D'Avino G, Greco F, Maffettone PL (2017) Particle migration due to viscoelasticity of the suspending liquid and its relevance in microfluidic devices. Annu Rev Fluid Mech 49:341–360

Davis JA et al (2006) Deterministic hydrodynamics: taking blood apart. Proc Natl Acad Sci USA 103:14779–14784

Del Giudice F, Sathish S, D'Avino G, Shen AQ (2017) "From the edge to the center": viscoelastic migration of particles and cells in a strongly shear-thinning liquid flowing in a microchannel. Anal Chem 89:13146–13159

Di Carlo D (2009) Inertial microfluidics. Lab Chip 9:3038–3046. https://doi.org/10.1039/B912547G

Faridi MA, Ramachandraiah H, Banerjee I, Ardabili S, Zelenin S, Russom A (2017) Elasto-inertial microfluidics for bacteria separation from whole blood for sepsis diagnostics. J Nanobiotechnology 15:3

Gossett DR et al (2010) Label-free cell separation and sorting in microfluidic systems. Anal Bioanal Chem 397:3249–3267

Hejazian M, Li W, Nguyen N-T (2015) Lab on a chip for continuous-flow magnetic cell separation. Lab Chip 15:959–970

Heyman JS (1993) Acoustophoresis separation method. J Acoust Soc America 94(2):1176–1177

Kang Y, Li D, Kalams SA, Eid JE (2008) DC-Dielectrophoretic separation of biological cells by size. Biomed Microdevices 10:243–249

Kang K, Lee SS, Hyun K, Lee SJ, Kim JM (2013) DNA-based highly tunable particle focuser. Nat Commun 4:2567

Khoo BL, Grenci G, Lim YB, Lee SC, Han J, Lim CT (2018) Expansion of patient-derived circulating tumor cells from liquid biopsies using a CTC microfluidic culture device. Nat Protoc 13:34

Kuntaegowdanahalli SS, Bhagat AAS, Kumar G, Papautsky I (2009) Inertial microfluidics for continuous particle separation in spiral microchannels. Lab Chip 9:2973–2980

Lee DJ, Brenner H, Youn JR, Song YS (2013) Multiplex particle focusing via hydrodynamic force in viscoelastic fluids. Sci Rep 3:3258

Leshansky A, Bransky A, Korin N, Dinnar U (2007) Tunable nonlinear viscoelastic "focusing" in a microfluidic device. Phys Rev Lett 98:234501

Liu C, Ding B, Xue C, Tian Y, Hu G, Sun J (2016) Sheathless focusing and separation of diverse nanoparticles in viscoelastic solutions with minimized shear. Thinning Anal Chem 88:12547–12553

Liu C et al (2017) Field-free isolation of exosomes from extracellular vesicles by microfluidic viscoelastic flows. ACS Nano 11 6968–6976

Lu X, Liu C, Hu G, Xuan X (2017) Particle manipulations in non-Newtonian microfluidics: a review. J Colloid Interface Sci 500:182–201

MacDonald M, Spalding G, Dholakia K (2003) Microfluidic sorting in an optical lattice. Nature 426:421–424

Magda J, Lou J, Baek S, DeVries K (1991) Second normal stress difference of a Boger. Fluid Polymer 32:2000–2009

McDonald JC, Whitesides GM (2002) Poly (dimethylsiloxane) as a material for fabricating microfluidic devices. Account Chem Res 35:491–499

Morton KJ, Loutherback K, Inglis DW, Tsui OK, Sturm JC, Chou SY, Austin RH (2008) Crossing microfluidic streamlines to lyse, label and wash cells. Lab Chip 8:1448–1453

Nam J, Shin Y, Tan JKS, Lim BY, Lim CT, Kim S (2016) High-throughput malaria parasite separation using a viscoelastic fluid for ultrasensitive PCR detection. Lab Chip 16:2086–2092

Nitta N et al (2018) Intelligent image-activated cell sorting. Cell 175:266–276.e213

Pamme N (2007) Continuous flow separations in microfluidic devices. Lab Chip 7:1644–1659

Pathak JA, Ross D, Migler KB (2004) Elastic flow instability, curved streamlines, and mixing in microfluidic flows. Phys Fluids 16:4028–4034

Sajeesh P, Sen AK (2014) Particle separation and sorting in microfluidic devices: a review. Microfluid Nanofluid 17:1–52

Seo KW, Byeon HJ, Huh HK, Lee SJ (2014) Particle migration and single-line particle focusing in microscale pipe flow of viscoelastic fluids. RSC Adv 4:3512–3520

Sollier E, Murray C, Maoddi P, Di Carlo D (2011) Rapid prototyping polymers for microfluidic devices and high pressure injections. Lab Chip 11:3752–3765

Vaidyanathan R, Yeo T, Lim CT (2018) Microfluidics for cell sorting and single cell analysis from whole blood. Methods Cell Biol 147:151–173

Whitesides GM (2006a) The origins and the future of microfluidics. Nature 442:368–373

Whitesides GM (2006b) The origins and the future of microfluidics. Nature 442:368

Xiang N, Dai Q, Ni Z (2016a) Multi-train elasto-inertial particle focusing in straight microfluidic channels. Appl Phys Lett 109:134101

Xiang N, Zhang X, Dai Q, Chen J, Chen K, Ni Z (2016b) Fundamentals of elasto-inertial particle focusing in curved microfluidic channels. Lab Chip 16:2626–2635

Yamada M, Nakashima M, Seki M (2004) Pinched flow fractionation: continuous size separation of particles utilizing a laminar flow profile in a pinched microchannel. Anal Chem 76:5465–5471

Yan S, Zhang J, Alici G, Du H, Zhu Y, Li W (2014) Isolating plasma from blood using a dielectrophoresis-active hydrophoretic. device Lab Chip 14:2993–3003. https://doi.org/10.1039/C4LC00343H

Yang S, Ündar A, Zahn JD (2007) Continuous cytometric bead processing within a microfluidic device for bead based sensing platforms. Lab Chip 7:588–595

Yang S, Kim JY, Lee SJ, Lee SS, Kim JM (2011) Sheathless elasto-inertial particle focusing and continuous separation in a straight rectangular microchannel. Lab Chip 11:266–273

Yuan D, Zhang J, Yan S, Pan C, Alici G, Nguyen N-T, Li W (2015) Dean-flow-coupled elasto-inertial three-dimensional particle focusing under viscoelastic flow in a straight channel with asymmetrical expansion–contraction cavity arrays. Biomicrofluidics 9:044108

Yuan D, Zhang J, Sluyter R, Zhao Q, Yan S, Alici G, Li W (2016a) Continuous plasma extraction under viscoelastic fluid in a straight channel with asymmetrical expansion–contraction cavity arrays. Lab Chip 16:3919–3928

Yuan D et al (2016b) Investigation of particle lateral migration in sample-sheath flow of viscoelastic fluid newtonian fluid. Electrophoresis 37:2147–2155

Yuan D et al (2017a) On-chip microparticle and cell washing using co-flow of viscoelastic fluid and Newtonian fluid. Anal Chem 89:9574–9582. https://doi.org/10.1021/acs.analchem.7b02671

Yuan D et al (2017b) Sheathless Dean-flow-coupled elasto-inertial particle focusing and separation in viscoelastic fluid. RSC Adv 7:3461–3469

Yuan D, Zhao Q, Yan S, Tang S-Y, Alici G, Zhang J, Li W (2018) Recent progress of particle migration in viscoelastic fluids. Lab Chip 18:551–567. https://doi.org/10.1039/C7LC01076A

Zeng J, Chen C, Vedantam P, Brown V, Tzeng T-RJ, Xuan X (2012) Three-dimensional magnetic focusing of particles and cells in ferrofluid flow through a straight microchannel. J Micromech Microeng 22:105018

Zhang J, Yan S, Yuan D, Alici G, Nguyen N-T, Warkiani ME, Li W (2016) Fundamentals and applications of inertial microfluidics: a review. Lab Chip 16:10–34